New Techniques of Low Level Environmental Radiation Monitoring at JLab

Pavel Degtiarenko and Vladimir Popov, *Thomas Jefferson National Accelerator Facility*

***Abstract*—We present the first long-term environmental radiation monitoring results obtained using the technique of pulse mode readout for the industry-standard Reuter-Stokes RSS-1013 argon-filled high pressure ionization chambers (HPIC). With novel designs for the front-end electronics readout and customized signal processing algorithms, we are capable of detecting individual events of gas ionization in the HPIC, caused by interactions of gammas and charged particles in the gas. The technique provides enough spectroscopic information to distinguish between several different types of environmental and man-made radiation. The technique also achieves a high degree of sensitivity and stability of the data, allowing long-term environmental radiation monitoring with unprecedented precision.**

***Index Terms*—Environmental radiation monitoring, ionization chambers, noise measurement, radiation detection circuits, signal processing**

I. Introduction

ENVIRONMENTAL radiation monitoring at the perimeters of radiation-generating installations in densely populated areas presents the challenge of measuring weak signals over the natural radiation background, which can be much larger than the signals of interest, and often vary with time. Continuous Electron Beam Accelerator Facility at Jefferson Lab is an example of such installation; it occupies a relatively small footprint in the midst of the Hampton Roads metropolitan area in Virginia. Strict administrative requirements limit the yearly operational radiation dose accumulation at the CEBAF boundary to no more than 10% of the natural background level, which is about 1 mSv. Until present, the precision necessary in the environmental measurements around CEBAF could only be achieved when measuring neutron skyshine signals at the boundary. Natural neutron background is small and we've been able to detect operational neutron dose rates at a level of about 1 nSv/h. The contribution of operational gamma dose was evaluated indirectly during special measurements. Direct continuous measurements and long-term monitoring of operational gamma dose rates at needed levels of sensitivity and stability were impractical due to cost and complexity of available solutions. Recently developed pulse-mode readout electronics for Ionization Chambers [1] allowed us to successfully make these measurements. HPIC hardware may be characterized as one of the most stable and reliable types of ionizing radiation detectors. The number of ion pairs produced by a radiation field in the fixed amount of gas filling the HPIC is independent of temperature and other environmental parameters. Ultimately reliable and stable charge collection and measurement in the low-level radiation fields may be achieved by using the pulse-mode operation of the readout electronics. The new schematics

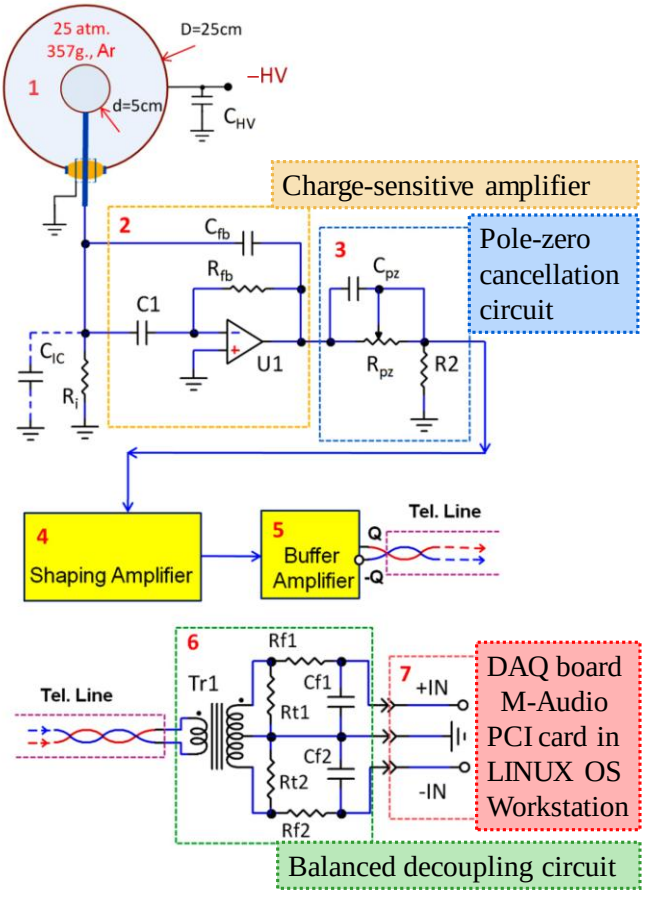

Fig. 1. Electronics circuit diagram for the pulse-mode readout front end to the GE Reuter-Stokes high pressure argon-filled Ionization Chamber.

Manuscript received May 15, 2009.

Notice: Authored by Jefferson Science Associates, LLC under U.S. DOE Contract No. DE-AC05-06OR23177. The U.S. Government retains a non-exclusive, paid-up, irrevocable, world-wide license to publish or reproduce this manuscript for U.S. Government purposes.

P. Degtiarenko is with the Radiation Control Department, Thomas Jefferson National Accelerator Facility, 12050 Jefferson Avenue, Suite 602, Newport News, VA 23606 (phone: 757-269-6274; fax: 757-264-6050; e-mail: pavel@jlab.org).

V. Popov is with the Radiation Control Department, Thomas Jefferson National Accelerator Facility, 12050 Jefferson Avenue, Suite 602, Newport News, VA 23606 (e-mail: popov@jlab.org).

allows the user to avoid widely known problems of the temperature-dependent voltage and current biases in the front-end electronics cascades, avoid complicated temperature compensating schematics, and avoid the need in frequent calibrations of the device, thus making the system practical. In addition to such stability, this novel detection system may provide extra information characterizing the energy distribution of the radiation field, helping to distinguish between several types of environmental and man-made radiation.

II. Front-End Electronics

The front-end electronics (see the diagram in Fig. 1) was upgraded as compared with [1] to achieve lower level of thermal noise by optimizing component base and adding new circuitry for the signal transmission. A twisted-pair telephone line carried amplified signals from the detector location at the boundary to the data acquisition computer at about 200 m distance. To allow for fast electron collection at the input, the HPIC [2] operated at minus 300 V bias voltage applied to the external shell. Balanced and decoupled output signals provided good protection from synphase and ground loop noise at the far end of the line.

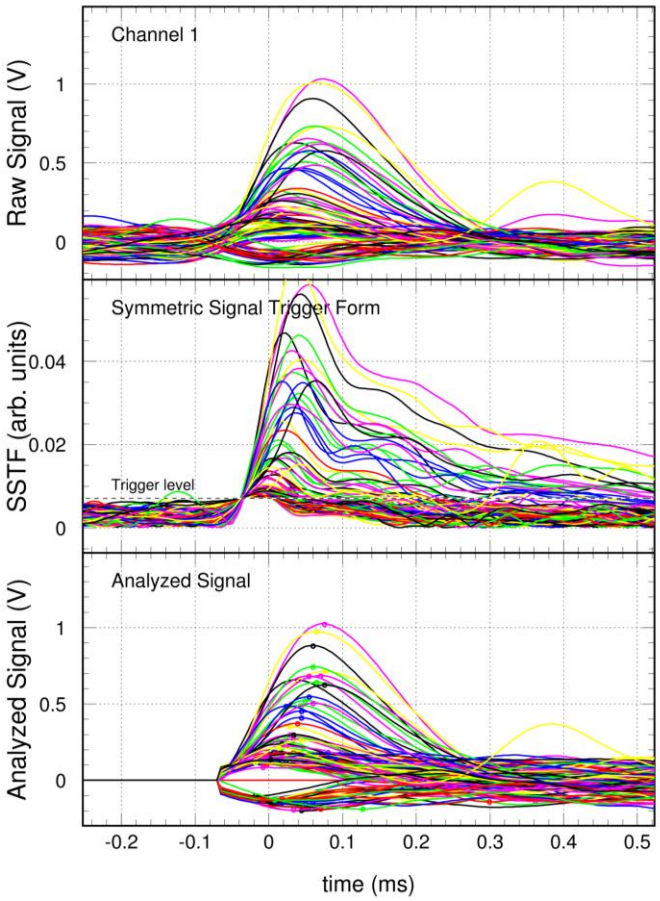

Fig. 2. Top panel: typical raw signals as recorded in the Wave file data stream, synchronized with the sign-symmetric trigger functions shown in the middle panel. Bottom panel shows corresponding analyzed signals with pedestal subtracted and positive or negative amplitude values found (shown by the dots at the top of each signal).

III. Signal Processing

An M-Audio Audiophile 192 High-Definition 24 bit audio PCI card [3] served as a wide dynamic range two-channel precision Analog to Digital converter operating at 192 kHz sampling rate.

A LINUX OS computer workstation capable of reading and analyzing continuously and simultaneously up to 3 such cards, served as a relatively inexpensive 6-channel data acquisition station, characterized by good stability and wide dynamic range. It is suitable for taking low rate signals from environmental detectors.

Data streams were accumulated as 10-minute standard Wave format audio files in the computer memory, and then analyzed using the Physics Analysis Workstation software from CERN [4] to find and analyze signals. Signal parameters were stored in the database and the raw files deleted to free memory. Fig. 2, top panel shows examples of about 100 raw signals in a regular run. The second panel shows corresponding "symmetric signal trigger form" functions for these signals. SSTF is a form built using the weighted combination of squared signal and time-shifted squared differentiated signal functions taken from the raw data file. Symmetric positive and negative signals produce identical SSTFs. This allowed us to evaluate the contribution of symmetric noise in the asymmetric (positive here) signal spectra from the HPIC. Fig. 2, bottom panel shows the same signals analyzed with the low frequency noise plateau subtracted and signal amplitude found (shown by the dots at the apex of each signal).

IV. Noise Subtraction

Possible sources of the signal noise at the end of the long transmission line, such as thermal noise contribution from the charge sensitive amplifier, microphonic effects of the HPIC sensitive to loud sounds in the environment, currents induced

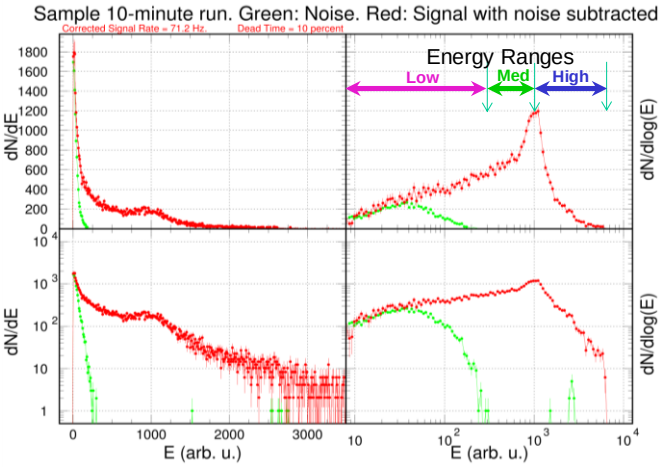

Fig. 3. Typical example of a signal spectrum from the HPIC, accumulated in a 10 min time interval, and shown in all combinations of linear and log scales. Arrows in the top right panel indicate three energy bands used in further analysis.

by the ground loops, etc., are characterized often by their random statistical fluctuations nature, and thus expected to be statistically symmetrical with respect to the sign of the current fluctuations. Symmetric trigger of the signal processing algorithm allowed us to measure directly and then statistically subtract the contributions of such noise from the signal spectra. Fig. 3 shows typical example of a signal spectrum accumulated in a 10-minute time interval. Four panels show the same event distributions in all combinations of linear and logarithmic scales, each underlining different aspects of the spectral shape. Energy scale is arbitrary, but crudely corresponding to keV deposited in argon.

Green distribution is the symmetric noise evaluated from the amplitude spectrum of the negative signals, and red distribution is the result of subtraction of the spectrum of all positive signals minus noise. We can see from the plots that the noise contribution, as expected, is concentrated at low energies, and falls sharply at energies above approx. 200 keV. The subtraction procedure allows us to use the low energy portion of the spectrum reliably and eliminate the temperature dependence of the detector output at low energies, observed in [1]. Another advantage is eliminating from the detector output rare, but noticeable events of loud sounds in the environment, such as overhead jet noise.

The spectra exhibit visible shoulder, or peak in the log distribution at energy about 1 MeV, corresponding to the contribution from cosmic muon flux. The contribution of the muon flux to the environmental dose rates is significant; as well significant are the statistical fluctuations in the muon rates, and its known [5] dependence on atmospheric parameters such as pressure and temperature. To better detect low level dose generated by CEBAF operations it is advantageous to treat low and high energy ranges separately.

V. Energy Spectra

Fig. 4 further illustrates the spectrometric ability of the new design. A series of measurements was performed using low activity point radioactive sources ^{57}Co, ^{22}Na, ^{60}Co, and ^{228}Th in the lab. The shapes of the spectra, with background subtracted, reflect major gamma energy lines present in different isotopes (^{57}Co source contained traces of isotopes producing higher energy gammas). We may conclude from these spectra that the new HPIC device may be used to characterize spectra of gamma radiation present in the environment with 30-50 % resolution and the dynamic range of about 100 keV to 3-6 MeV.

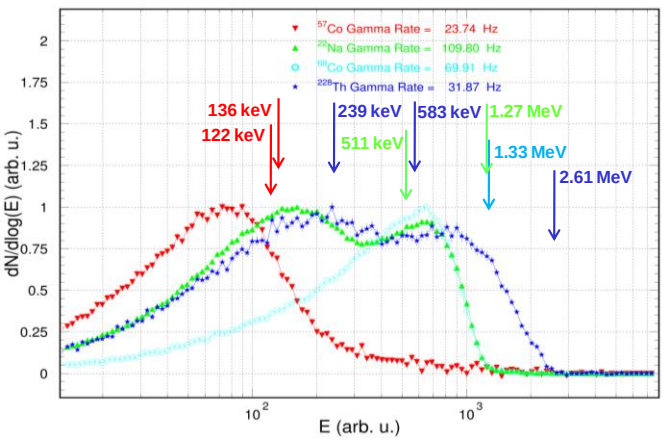

Fig. 4. Four distributions shown correspond to four test runs in the lab when different low intensity radioactive isotopes were used to irradiate the HPIC. Arrows indicate energy of the gamma lines characteristic for ^{57}Co, ^{22}Na, ^{60}Co, and ^{228}Th. Event rates during the tests are shown in the plot. All spectra are normalized to have their maxima at 1.

VI. Calibration

Two spectroscopic HPIC detectors were set up at CEBAF boundary, one at the location closest to the experimental Halls (RBM-3, stands for "Radiation Boundary Monitor 3"), and the other (RBM-6) serving as a reference. The calibration procedure involved day-long runs in January, 2009 with a low activity point ^{228}Th source placed at the detectors in identical positions, and adjusting calibration factors to achieve equal response of the detectors to the same dose of about 40 nSv/h distributed in three energy bands. This procedure is illustrated in Fig. 5.

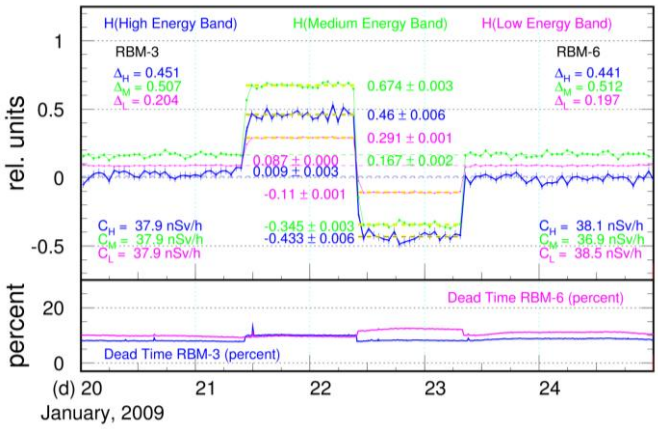

Fig. 5. Illustration of the calibration procedure. Top panel shows the difference between the non-calibrated readouts from the two detectors, RBM-3 and RBM-6, plotted against time for five days before, during, and after runs when the calibration source was installed first in RBM-3, and then in RBM-6 in identical positions. Symmetric response around the base lines indicates that in all three energy bands the calibration factors are selected correctly. Straight dashed lines correspond to the average levels measured during these periods, with values shown. The Δ parameters for RBM-3 and RBM-6 detectors show the rate increases for the corresponding detector in the three energy ranges during the test, and the C parameters represent final calibration parameters to be applied to convert non-calibrated detector readings into dose rate in nSv/h. Bottom panel shows corresponding detector dead times during the tests (dead time correction is done automatically online).

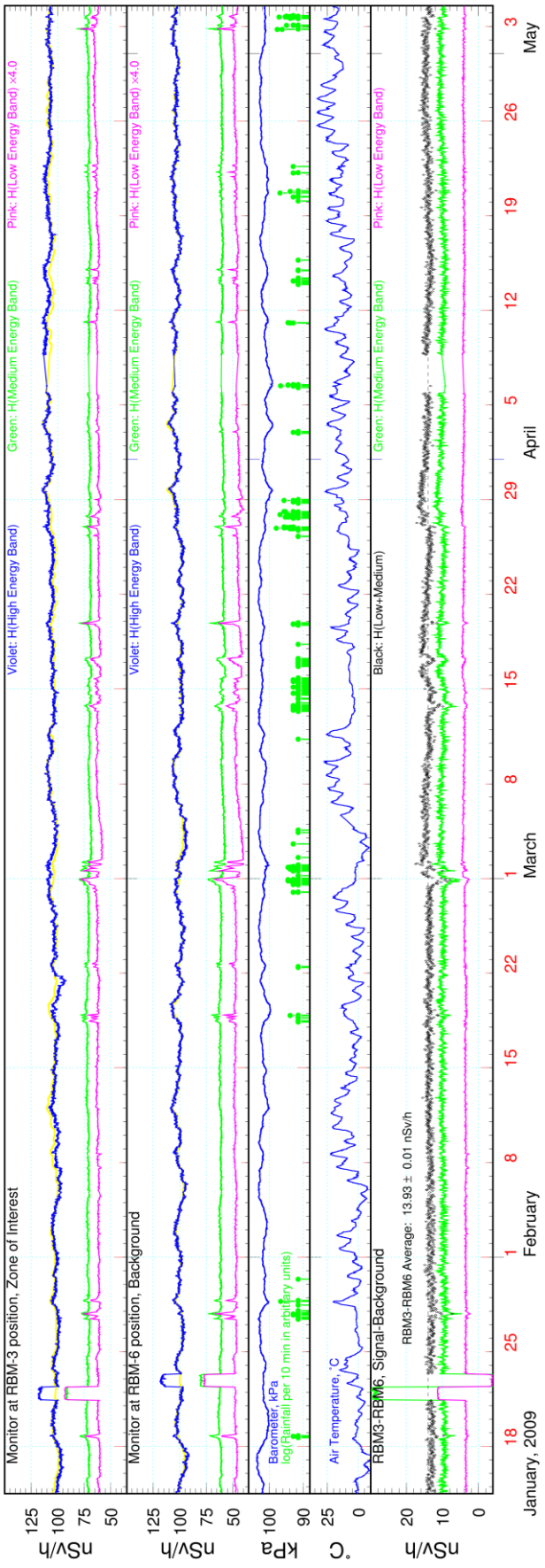

Fig. 6. Time histories plots. See Fig. 7 caption and text for details.

VII. Time Histories

Continuous measurements at the CEBAF site boundary were started in mid-January, 2009, running without major interruptions and without extra adjustments from then on. Figs. 6 and 7 show the examples of time histories of the two detectors' hourly readouts during the first few months in 2009, including the calibration procedure on January 21-23. During that time period there were no significant accelerator operations. During the period of about two weeks in November and December of 2009, 6 GeV electron beam current was delivered to one of CEBAF's Experimental Halls. Dose rates measured in low (L), medium (M), and high (H) energy bands are shown for RBM-3 and RBM-6 locations in the upper two panels. The following two panels show atmospheric pressure and temperature together with the rainfall data. The bottom panel presents the difference between the two detectors, in the low, medium, and (low + medium) energy ranges, as a function of time. Among the general regularities observed in the data, we list the clear anticorrelation of the H band readouts with the atmospheric pressure, as well as the visible rain effects in the L and M bands. Similar effects were observed in earlier investigations (see [5] and references there). Non-zero average difference and different response of the detectors to rain are due to

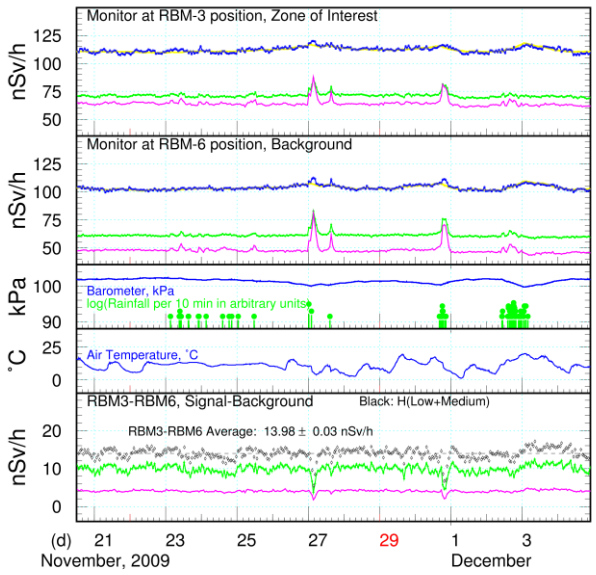

Fig. 7. Same as Fig. 6, showing the period of about two weeks in November and December, 2009, with the accelerator operations under way. Hourly readouts from the HPICs at the RBM-3 position, zone of interest close to the experimental Halls, and at the RBM-6 position, background site further away, are plotted as a function of time in the top two panels. Dose rates measured in Low, Medium, and High energy bands are shown with pink, green, and violet lines (positioned in the lower, medium, and upper portions in these panels). Low energy band data are shown in the plot multiplied by a factor 4.0 to better fit in the panels. Third and fourth panels provide the weather information, such as barometric pressure, air temperature, and rainfall during the period. The bottom panel shows the difference between the HPICs at RBM-3 and RBM-6 positions in the Low and Medium energy bands (pink and green lines). Black series of points represents the sum of the Low + Medium energy bands.

different soil conditions in the two locations. The long term stability of the readouts can be judged visually from the difference plots which stay within a few nSv/h at the base level of 80-90 nSv/h for the sum of L+M energy bands. To achieve precise measurements and realize the ultimate sensitivity of the difference method in the future setups would require special preparations of the monitoring sites to make their local environmental conditions (such as soil composition, detector placement, etc.) as identical as possible.

The stability of the difference between the HPIC monitors in RBM-3 and RBM-6 position during dry periods permits observation of very small dose rate contributions from the accelerator operations. This fact is illustrated in Fig. 8.

High power 6 GeV electron beam was delivered to the semi-underground experimental setup in Hall A at JLab, approx. 150 meters away from the RBM-3 position during the same time period in November and December of 2009. The difference of readouts of RBM-3 and RBM-6 detectors is shown correlated with the neutron dose rate measured at RBM-3 position, and with the high power beam current delivered to Hall A. Scheduled and opportunistic beam interruptions, indicated by the absence of the current data and low values of the neutron dose rate, allowed the determination of the background level in the HPIC measurements (shown by the black solid dots). Red (open) circles correspond to hours with the beam on, and are used to evaluate the contribution of the accelerator operations to the ionizing radiation at the boundary. The average dose rate attributed to the accelerator operations during this period (about 3.5 nSv/h) is shown by the red dashed line. Thus, we may conclude that we reliably observe the contribution of the dose rate at the boundary produced by the accelerator operations at the level of about 1-1.5 percent of the natural radiation background at JLab (corresponding to the sum of L+M+H bands of approx. 180-200 nSv/h).

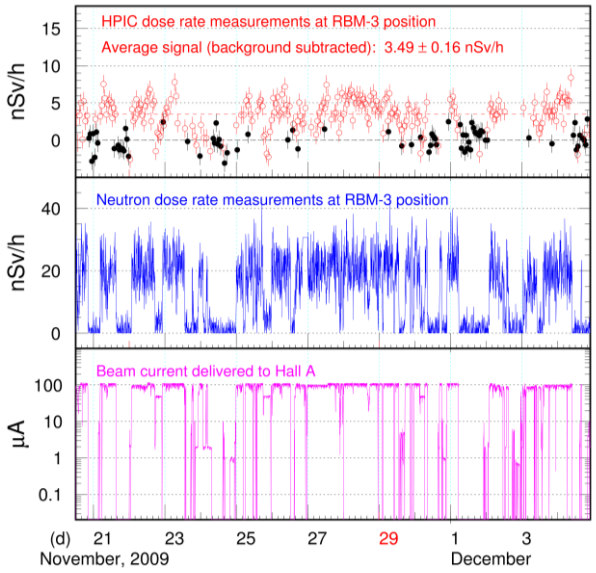

Fig. 8. Radiation dose rates at the RBM-3 position at JLab boundary as measured by the HPICs (top panel) and the environmental neutron dose rate monitor (see [6] and references there) at the same position (middle panel), correlated in time with the accelerator beam current delivery to one of the experimental halls at JLab (bottom panel). Hours during and immediately following a rainfall are not included in the analysis.

VIII. Conclusions

Long-term operation of this new type of sensitive and stable environmental radiation monitoring and spectroscopic system has been demonstrated, based on the industry-standard argon-filled HPIC with novel pulse-mode readout of front-end electronics and novel signal processing algorithms. Low level gamma dose rates in three energy bands at two locations around CEBAF were measured continuously for over 10 months. Dose rate variations at the level of a few percent are clearly seen in the data, correlated with atmospheric pressure and rainfall. The difference between the two probes, characterizing radiation produced by the machine operations, is observed to be stable and sensitive down to a level of about 3-5 nSv/h measured in an hour, and much better if integrated.

Acknowledgment

This work is supported by the Radiation control Department, ESH&Q Division at Jefferson Lab. The authors thank R. May and V. Vylet for their interest and support of this study.

References

[1] *V. Popov, P. Degtiarenko*: "Pulse-Mode Readout Electronics for Ionization Chambers", IEEE TRANSACTIONS ON NUCLEAR SCIENCE, VOL.56, NO.3, JUNE 2009.

[2] "RSS-131ER Environmental Radiation Monitor", Available: http://www.gepower.com/prod_serv/products/radiation_monitors/en/downloads/rss131.pdf

[3] M-Audio Audiophile 192 Audio Card, Available: http://www.maudio.com/products/en_us/Audiophile192-main.

[4] *R. Brun, O. Couet, N. Cremel, A. Nathaniel, A. Rademakers, C. Vandoni*: "PAW – Physics Analysis Workstation Package", CERN Program Library entry Q121, CERN, Geneva, 1988.

[5] *F. Wissmann*: "Variations Observed in Environmental Radiation at Ground Level", Radiation Protection Dosimetry (2006), Vol. 118, No.1, pp. 3-10.

[6] *P.Degtyarenko, D.Dotson, R. May, S. Schwahn, G. Stapleton*: "Initial Measurements of Site Boundary Neutron Dose and Comparison with Calculations", in: Proceedings of the Health Physics Society 30-th Midyear Topical Meeting on Health Physics of Radiation-Generating Machines, 5-8 January 1997, San Jose, California, p.205-212.